Egyptian Journal of Chemistry

Fixed -Bed column studies for the adsorption of crystal violet over resorcinol- formaldehyde xerogel and carbon nanotubes nanohybrids

Amina A. Attia, Nady A. Fathy*, Mona A. Shouman,
Physical Chemistry Department, Research Institute of Advanced Materials Technology and Mineral Resources, National Research Centre, 33 El Bohouth Street (former Tahrir St.), Dokki, Giza, P.O. 12622, Egypt

Abstract

The adsorption performance of multiwalled carbon nanotubes (MWCNTs), resorcinol-formaldehyde xerogel/CNTs (RFX/MWCNTs), and its hydrothermally carbonized sample (C-RFX/MWCNTs) towards the removal of crystal violet (CV) dye using a fixed bed column is investigated. The produced samples were characterized with TEM, FTIR, and N_2 adsorption tests. In terms of CV adsorption performance, the impact of flow rate, bed height, and intake concentration on breakthrough curves was evaluated. To forecast column performance, the Wolborska, Adam-Bohart, and Clark models were being used. MWCNTs have typical sizes ranging from 30 to 60 nm, according to TEM analysis. C-RFX/MWCNTs displayed more oxygenated functional groups as well as an increase in internal porosity after hydrothermal carbonization. The capacity of the adsorption bed increased with increasing bed height, reducing flow rate, and decreasing initial dye concentration, according to the results of the column. The findings of the experiments revealed that the hydrothermally carbonized sample (C- RFX/MWCNTs) is a quite effective adsorbent for uptaking the crystal violet dye.

Keywords: Nanohybrids, carbon nanotubes, carbon xerogels, crystal violet dye, column studies

1. Introduction

Carbon xerogels (CXs) composed of three-dimensional network interconnected nodules as carbon nanostructures exhibit attractive properties including low mass density, high surface area, and high conductivity [1-5]. Moreover, CXs materials can easily be combined with some additives such as metals and carbon nanotubes (CNTs) to improve their surface characteristics [6].

Carbon nanotubes (CNTs) have been studied extensively in recent decades and showed exceptional features such as low weight, large surface area, chemical stability, good thermal and electrical, and mechanical strength properties [7-10]. CNTs are a good choice for environmental applications such as sorption, filtration, and separation due to their exceptional features. In order to enhance the adsorption capability and electrochemical property of CNTs, several methods such as functionalization and surface modification with carbon gels have been proposed [11-18]. Tabrizi and Yavari [11] fabricated CNTs and carbon aerogels for removing methylene

blue dye from aqueous solutions. They found that CNTs-based carbon aerogels with higher specific surface area and adsorption capacity of methylene blue dye than that of carbon aerogels only. Worsley et al. [12] synthesized a monolithic of double-walled carbon nanotubes (DWCNTs)/carbon aerogels nanocomposites during sol-gel polymerization of resorcinol and formaldehyde in an aqueous solution containing a surfactant stabilized dispersion of DWCNTs. In a further investigation, they studied properties of single-walled carbon nanotubes-based carbon aerogels as a function of nanotube loading (0 − 55 wt%) [13]. Earlier research by Haghgoo et al. [14] documented the preparation of multi-walled carbon nanotubes (MWCNTs) dispersed in resorcinol-formaldehyde (RF) aerogel using sodium dodecyl benzene sulfonate and studied the dispersion effect of MWCNTs on the final properties of RF matrix. Also, Haghgoo and coworkers [15] studied the correlation between morphology and electrical conductivity of dried and carbonized multi-walled carbon nanotube/resorcinol– formaldehyde xerogel

composites, where the maximum surface area of the MWCNTs/carbon xerogels (CXs) reached to 685 m^2/g. Fathy et al. [16] synthesized carbon nanotube/carbon xerogel hybrid (CNT/CX) during chemical vapor decomposition of camphor in presence of RF xerogel loaded with nickel catalyst. Results showed that this hybrid exhibited a specific surface area of 95 m^2/g and a maximum capacitance of 50 F/g. Therefore, incorporating of CNTs into the carbon gels matrix through sol-gel step can produce valuable nanohybrids accompanying with an improvement in their chemical, electrical, thermal and mechanical properties. On the basis of these promising findings, the nanohybrids consisting of carbon xerogel and carbon nanotubes (CX/ CNTs) were used effectively as electrodes in an energy storage application [15–18]. In a further recent work, Shouman and Fathy [19] prepared microporous nanohybrids of carbon xerogels and MWCNTs to investigate their adsorptive and catalytic oxidation behaviors towards removal of rhodamine B dye (RB). Results showed that the N_2 uptake was enhanced when CX was decorated with MWCNTs and the specific surface area (S_{BET}) was increased from 192 to 643 m^2/g.

Recently, few studies were carried out to prepare low cost CNTs using agricultural wastes [20, 21]. In this study, synthesized multiwalled carbon nanotubes (MWCNTs) from chemical vapor deposition of camphor over carbonized rice straw as natural substrate [20] were successfully used as additives with resorcinol-formaldehyde organic xerogel and then post treated under hydrothermal conditions for a comparison's sake.

Batch adsorption is a simple technique to utilize in the laboratory for treating small volumes of effluents, but it is more difficult to apply on an industrial scale, where vast volumes of wastewater are created on a regular basis. Batch adsorption gives preparatory knowledge such as the particle size for optimum pollutants adsorption, the optimal pH for maximum adsorption and the adsorbents adsorption capabilities. All of these stuffs are beneficial to fixed-bed research. The adsorbate is continuously in contact with a given quantity of raw adsorbent in a fixed-bed, resulting in the requisite concentration gradients among the adsorbent and the adsorbate for adsorption. Utilization of wastewater through percolating material is often used in fixed-bed adsorption of contaminants [22]. The wastewater is disinfected through physicochemical processes as it overflows through the percolator. The shape of the breakthrough curve (BTC) and its velocity through the bed are crucial to the design and theory of fixed-bed adsorption systems. In most cases breakthrough and bed volumes are used to assess the performance of a fixed-bed column [23]. The BTC is a motion that defines the performance of backed beds.

The aim of this work was to compare the column adsorption performance of the following samples; MWCNTs prepared in laboratory [20], resorcinol-formaldehyde organic xerogel (RFX) /MWCNTs nanohybrids prepared according to method as reported previously [19] and its counterpart that was post-heated under hydrothermal carbonization at 180ºC for 3 h to prepare carbonized sample from RFX/MWCNTs composite knowing as C-RFX/MWCNTs. The characteristics of MWCNTs, RFX/MWCNTs, and C-RFX/MWCNTs samples were studied and compared using TEM, FTIR and N_2 adsorption measurements. Crystal violet dye (CV) is being used as a model compound to assess the ability of produced samples to eliminate this dye through fixed bed columns and to evaluate the possibility of using such samples as a cost-effective adsorbent in an industrial setting. The performance and shape of the breakthrough curves (BTCs) were analyzed in relation to initial dye concentration, bed height and flow rate. Wolborska, Adam-Bohart and Clark were practiced to characterize the dynamic performance of the adsorption process.

Experimental

2.1. Materials

Resorcinol (C_6H_6O, Panreac, 99%), formaldehyde (HCHO, Adwic, 36-38%), methanol (CH_3OH, Adwic, 95%), sodium hydroxide (NaOH, SDFCL, 98%), sodium carbonate (Na_2CO_3, POCH SA, 99%), and cetyltrimethylammonium bromide (CTAB, Sigma-Aldrich, 99%) as cationic surfactant to help in dispersing MWCNTs through sol-gel process, were purchased and used without prior purification.

2.2. Preparation of MWCNTs

Laboratory MWCNTs sample was fabricated during chemical vapor deposition of camphor as carbon source onto a hydrothermally treated rice straw loading with iron and nickel oxides at 850ºC for 30 min [20]. The MWCNTs were washed with 6 M HCl to remove the catalyst and then purified with concentrated HNO_3 to remove the amorphous carbon particles.

2.3. Preparation of resorcinol-formaldehyde xerogel /MWCNTs nanohybrids

A sol-gel procedure of resorcinol-formaldehyde xerogel/MWCNTs was performed in presence of CTAB as cationic surfactant and Na_2CO_3 as alkaline catalyst (C) were dissolved in distilled water (W). Then a portion of formaldehyde solution (F) stabilized by 10 % methanol was added into this mixture under vigorous stirring to form the hydrogel. The obtained hydrogel was obtained after 30 min at 80ºC. The molar ratios of the used reactants with respect to resorcinol were calculated as; R/F= 0.5, R/C= 1000, and R/W= 0.027 and MWCNTs/CTAB=1/3. The pH of the sol was adjusted to 6.0 by 0.1 M NaOH solution. The

prepared hydrogel was then transferred into a stoppered glass bottle and heated in an air-oven at 80°C for 24 h to complete curing and gelling process. Afterwards, the sealed bottle was opened to allow the gel obtained for drying at the same temperature for another 48 h. The monolithic product of gel is labelled as RFX/MWCNTs.

Furthermore, a novel approach was performed using hydrothermal carbonization of RFX/MWCNTs sample in cylindrical stainless steel autoclave reactor at 180°C for 3h to produce carbonized sample known as C-RFX/MWCNTs.

2.4. Characterization tools

The morphology of the prepared samples was determined using high resolution-transmission electron microscope (HR-TEM, JEM-1230, Japan) operated at 120 kV. Fourier transforms infrared (FTIR) spectroscopy to give the main functional groups on the obtained samples was done using a KBr disk technique and FTIR 6500 spectrometer (JASCO, Japan) in the range of 400-4000 cm^{-1}. The textural properties such as Brunauer-Emmett-Teller surface area (S_{BET}, m^2/g), total pore volume (V_P, cm^3/g) and average pore diameter (R_P, nm) were measured using nitrogen adsorption analysis at -196°C (BEL-Sorp-max, MicrotracBel Crop, Japan) with analyzing pore size distributions which developed in the samples.

2.5. Dynamic adsorption studies

2.5.1. Adsorbate

Crystal violet dye (CV) used in this investigation was acquired from Sigma-Aldrich and utilized without any additional purification. About 0.05 g of dye was dissolved in 1 L of doubled distilled water to make a stock dye solution (50 mg/L).

2.5.2. Up-flow adsorption experiments in a fixed-bed

On a bench scale column set-up, the adsorption tests were carried out. A glass column with an internal diameter of 1 cm and a total height of a 50 cm, a rotameter, and a pump comprise the experimental set-up. CV stock solution (50 mg/L) was prepared. The effluent was assembled in individual test tubes. The impact of influent concentration (50 and 25mg/L), flow rate (5 and 7 mL/min) and bed depth (2 and 1 cm) on CV adsorption in the column was studied. The tested samples were analyzed using a UV-vis spectrophotometer (Shimadzu Model PC-2401) with 1.0 cm length –path cell by for measuring the maximum absorbance at a wavelength of 590 nm was applied to analyze the tested samples. All of these experiments were carried out at 25°C.

2.5.3. Determination of column parameters

The breakthrough curves in the fixed-bed adsorption system were designed as the ratio of effluent CV (C_t, mg/L) concentration to influent (C_o, mg/L) CV concentration (C_t/C_o) versus time (t, min). The parameters were expressed using the breakthrough time (t_b, min) is the point when the ratio between influent concentration and effluent concentration becomes 0.05 to 0.09, i.e., 50% breakthrough of the column, and saturation time (t_e, min), the CV concentration in the effluent attained 99% of the initial CV concentration. The column will be completely exhausted when the predetermined influent concentration is nearly equal to effluent concentration. The continuous flow adsorption data was analyzed using the equation below.

The effluent volume (V_{eff}, mL) can be approached from the following equation [24]:

$$V_{eff} = F\, t_e \qquad (1)$$

where F is the volumetric flow rate (mL/min).

At a particular flow rate and influent concentration, the total adsorbed quantity of dye (q_{total}, mg/g), defined as the area found above the breakthrough curve; was calculated using equation:

$$q_{total} = \frac{F}{1000} \int_{t=0}^{t=t_e} (C_o - C_t)\, dt \qquad (2)$$

where C_o and C_t are the influent and effluent dye concentrations (mg/L), respectively.

The total amount of dye that flows through the column is determined from equation:

$$m_{total} = \frac{C_o \times F \times t_e}{1000} \qquad (3)$$

The maximum capacity uptake of the column was attained from equation:

$$q_e = q_{total}/m \qquad (4)$$

where m is the dry weight of the adsorbent in the column (g). Equation (5) can be used to calculate the unsorbed CV dye concentration at equilibrium in the fixed bed column as follows:

$$C_{eq} = \frac{m_{total} \times q_{total}}{V_{eff}} \qquad (5)$$

The total CV removal efficiency is defined using equation:

$$\% \text{ removal} = \frac{q_{total} \times 100}{m_{total}} \qquad (6)$$

2.5.4. Column modeling data

The prediction of the column, breakthrough or the shape of the adsorption wave front, is the most significant parameter in the design of a column adsorber, since indicates the bed length, operating life span, and regeneration time. A hypothesis of the effluent's concentration time profile or breakthrough curve is required for the proper design of a column adsorption process. An adsorption column is designed using a variety of models. The models that were employed in this research are Wolborska, Adam-Bohart and Clark models.

Wolborska model [25]:

Wolborska model, which is used to describe the breakthrough curve in the low concentration range, was utilized to conduct an analysis of adsorption-column performance. This model depicts the concentration-distribution in the bed by equation:

$$\ln (C_t/C_o) = \frac{\beta\, C_o}{N_o} t - \frac{\beta Z}{U} \qquad (7)$$

where, β is the kinetic coefficient of external mass transfer (min^{-1}) which reflects the effects of mass

transfer in both the liquid phase and axial diffusion. N_o is the saturation concentration (mg/L), U is the superficial fluid velocity (cm^3/min) and Z is the height of fixed-bed (cm). The BTCs were linearized using Wolborska model by graphing ln (C_t/C_o) vs. t.

Adam-Bohart model [26]:

This model is based on surface reaction theory, and is widely employed to describe the initial part of breakthrough curves. This model speculates that the rate of adsorption is proportional to both the residual capacity of the adsorbent and the concentration of adsorbed species. The mathematical equation can be determined as following:

$$ln\ (C_t/C_o) = K_{AB}C_o\ t - K_{AB}\frac{N_oZ}{F} \quad (8)$$

where C_o and C_t are the influent and effluent concentrations of CV dye (mg/L), respectively. K_{AB} is the mass transfer coefficient (L/mg.min), Z is the bed height of the column (cm) and F is the superficial velocity of the influent concentration and identified as the ratio of volumetric flow rate (Q, cm^3/min) to the cross-sectional area of the bed (A, cm^3). These parameters were calculated from the intercept and slope of linear plot of ln (C_t/C_o) vs. t. If the coefficient K_{AB} is equal to β/N_o, the Wolborska model is comparable to the Adam-Bohart model. As a result, the parameters for both models were calculated using the identical plots of ln (C_t/C_o) against time (t, min) at a given flow rate, bed height and initial dye concentration.

Clark model [27]:

The Clark described a new initiation of breakthrough curves [28, 29]. This model is primarily based totally at the mass transfer coefficient in combination with the Freundlich isotherm.

$$ln\ [(\frac{C_o}{C})^{n_f-1}-1] = ln\ A - r.\ t \quad (9)$$

Where, C_t is the effluent concentration (mg/L), C_o is the influent concentration (mg/L), A and r are both Clark constants (min^{-1}), n_f is the Freundlich constant, and t is the time (min). Equation 9 was employed to the effluent data for the fixed bed adsorbing applying linear regression. The Freundlich constant (n_f) was used to determine the parameters in the Clark model. From a plot of $[(C_t/C_o)^{n-1}-1]$ vs. t, the value of r (1/min) and A can be thus calculated from its slope and intercept respectively (Fig. 7a, b,c).

3. Results and discussion
3.1. Morphology and surface features of samples

To follow the change in morphology of RFX, MWCNTs, RFX/MWCNTs and C-RFX/MWCNTs, TEM technique is done. As expected in morphology of RFX, the material is composed of interconnected nodules of carbon spheres with sizes varied between 20 and 50 nm (Fig. 1A). In Fig. 2B, straight tubes of MWCNTs with outer diameters ranged from 30 to 60 nm were obtained. Combination of RFX and MWCNTs through sol-gel process in presence of

CTAB surfactant is shown in Fig. 1C, indicating the distribution of carbon nodules on surface of CNTs which results in minimizing the interconnection between nodules of RFX. TEM of C-RFX/CNTs (Fig. 1D) showed unlike morphology as a result of further hydrothermal treatment. It can be seen a substantial gathering of nodules on longitude tubular of MWCNTs with bending in these tubes.

To explain the changes in the surface chemistry of prepared samples, FTIR spectrum tool was used. FTIR spectra of MWCNTs, RFX/MWCNTs and C-RFX/MWCNTs are illustrated in Fig. 2. FTIR spectrum of MWCNTs sample showed peaks at 1725, 1623, 1029, 3429, 2832 and 2922 cm^{-1} which can be assigned to C=O and C=C stretching C–O, OH stretching of the carboxylic acid group, asymmetric and symmetric H-C stretching of H-C=O in the carboxyl group, respectively [21, 30]. The band appeared at 590 cm^{-1} is related to C-H out-of-plane bending vibrations in the aromatic ring. After combination of MWCNTs with RFX, the intensity of these bands increased except band at 1725 is disappeared that may confirm the attraction between RFX and MWCNTs through those functional groups [21]. Thus, the hydrothermal treatment inserted a large amount of oxygen containing-functional groups onto RFX/MWCNTs.
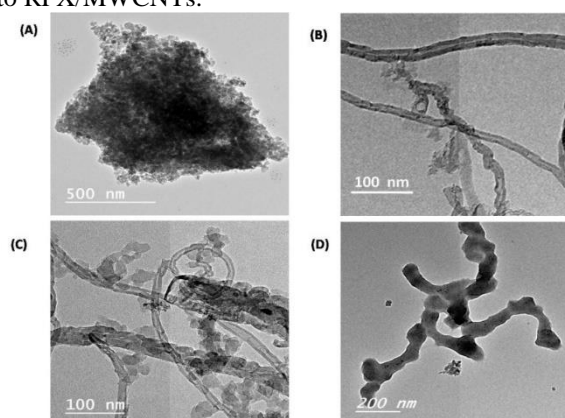

Figure 1: TEM images of the prepared samples of (A) RFX, (B) MWCNTs, (C) RFX/MWCNTs and (D) C-RFX/MWCNTs.
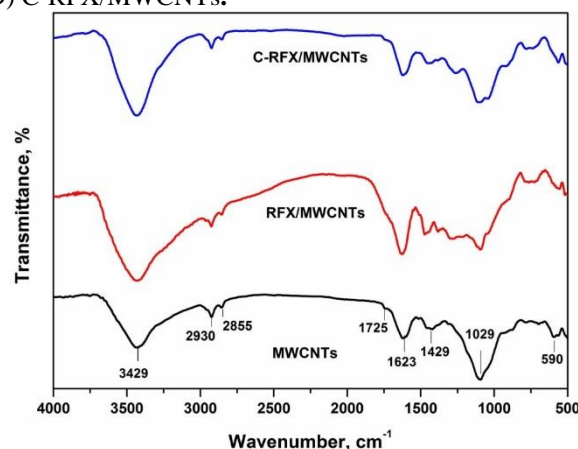
Figure 2: FTIR spectra of MWCNTs, RFX/MWCNTs and C-RFX/MWCNTs.

3.2. Textural properties of the samples

Fig. 3 shows the N_2 adsorption-desorption onto the studied samples. Table 1 summarizes the calculated porous parameters. The N_2 isotherms exhibit different shapes for uptaking nitrogen by MWCNTs as compared to that adsorbed by RFX/MWCNTs and C-RFX/MWCNTs, confirming the effect of preparation conditions on the porosity characteristics during sol-gel of RFX or post-carbonization through hydrothermal carbonization at 180ºC for 3h. The uptake of N_2 increased as in the following order: C-RFX/MWCNTs>RFX/MWCNTs>MWCNTs with increasing in mesopore volume while size of mesopore decreased forming narrow mesopores when RFX/MWCNTs sample was exposed to thermal treatment as shown in NLDFT pore size distributions plots (Fig. 3B). As clearly seen in Table 1, the porous properties of MWCNTs improved greatly when combined with resorcinol-formaldehyde xerogel (RFX) and when heated hydrothermally at 180ºC for 3h. It was found that the total surface area and total pore volume are increased substantially from 35 m^2/g and 0.069 cm^3/g for MWCNTs to be 477 m^2/g and 0.738 cm^3/g for C-RFX/MWCNTs. These findings affirm the high porosity character of C-RFX/MWCNTs and thus this would enhance the adsorption properties in the column adsorption of CV dye.

Table 1: Textural properties of the prepared samples.

Samples	S_{BET} (m^2/g)	V_P (cm^3/g)	R_P (nm)
MWCNTs	35	0.069	10.6
RFX/MWCNTs	155	0.560	14.4
C-RFX/MWCNTs	477	0.738	6.19

3.3. Dynamic adsorption studies
3.3.1. Performance of column under various operating conditions

The bed height, flow rate and initial influent concentration are the most relevant parameters for a breakthrough curve investigation. These parameters were explored for their influence on the shape of the breakthrough curve and column performance.

3.3.2. Effect of flow rate on the performance for CV uptake

In the fixed bed column adsorption process, the flow rate is essential. In the current study, the flow rate of CV dye solution was varied between 5 and 7 mL/min, while maintaining the bed height of 2 cm, and inlet concentration of CV dye in the feed at 25mg/L. The breakthrough curves are shown in Fig. 4, and the data from the adsorption column are described in Table 2. The column was depleted earlier for the three tested samples when the flow rate was higher. With a higher flow rate, the front of the mass transfer zone quickly approached the column's exit, leading to a lower removal percentage and dye

uptake. However, when the rate flow is low, the process was controlled by external mass transfer, which was also appropriate for intraparticle diffusion system. As a result, the diffusion process was more effective and sorbent's residence time was longer, which ultimately resulted in breakthrough time (t_b, min), saturation time (t_e, min) and high percentage removal [30].
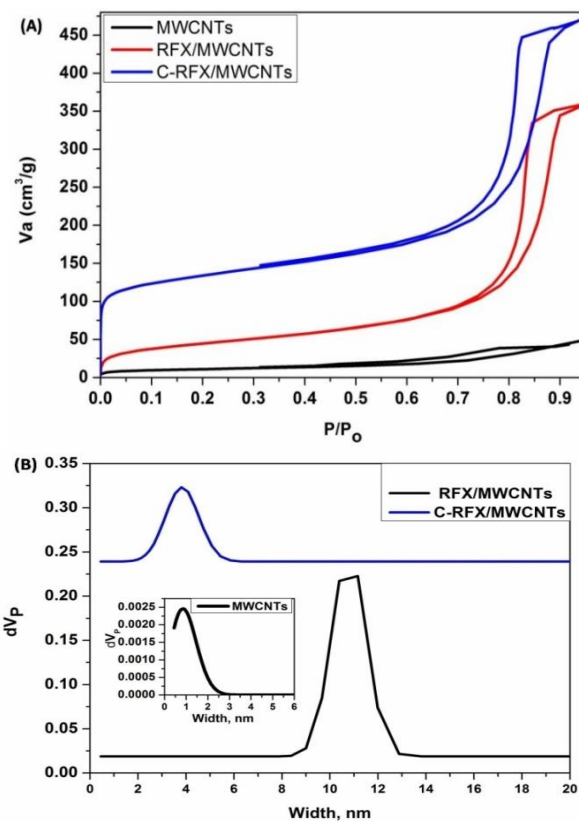

Figure 3: (A) N_2 adsorption/desorption isotherms and (B) NLDFT pore size distributions plots for the prepared samples.
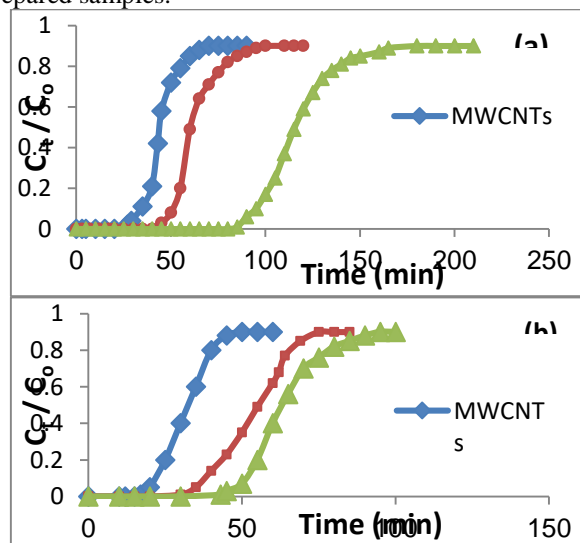

Figure 4: BTCs for the adsorption of CV by tested samples at different flow rates of (a) 5 and (b) 7 ml/min.

3.3.3. Effect of bed height on the performance removal of CV dye

The amount of adsorbate inside a fixed bed column determines the quantity of adsorbate accumulated, and the steepness of all breakthrough curves (BTCs) is a strong function of bed height. Fig. 5 shows the performance of BTCs at bed heights of 2 and 1 cm, while maintaining a flow rate of 5 mL/min and CV dye concentration of 25mg/L. Table 2 explains the relevant information gathered from these BTCs. As illustrated in Fig. 5, the breakthrough time (t_b, min) increased with increasing bed height for all of the examined samples. The residence time of CV dye solution inside the column increased as the bed height increased, enabling dye molecules to diffuse deeper into the adsorbents and resulting in higher removal capability. Table 2 clearly depicts that as bed height was increased, the breakthrough time (t_b, min) and exhaustion time (t_{ex}, min) were increased. This is owing to axial dispersion phenomena predominated at lower adsorbent bed heights, reducing CV adsorbate diffusion. Due to an increase in surface area of the adsorbents which supplied more binding sites for the adsorption, thus higher adsorption was seen at the maximum bed height [31, 32].
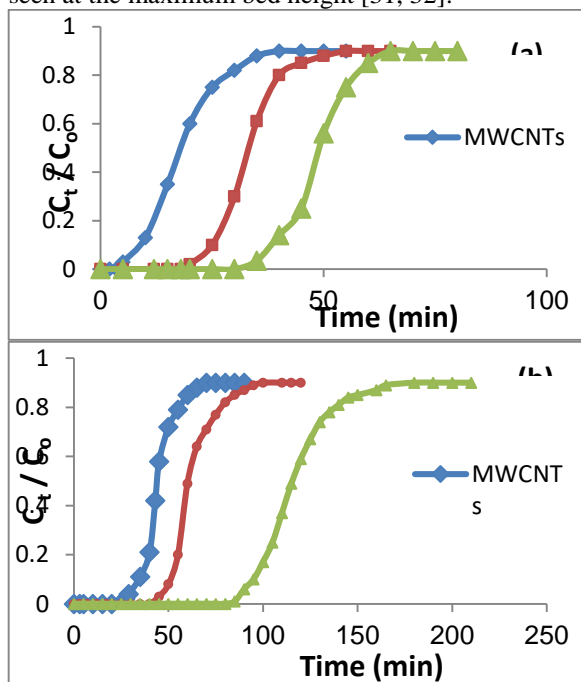

Figure 5: BTCs for the adsorption of CV by tested samples at different bed heights of (a) 1 and (b) 2 cm

3.3.4. Column adsorption properties of samples

From column parameters data, order of CV dye removal was C-RFX/MWCNTs> RFX-MWCNTs>MWCNTs. This trend of removal is observed due to the more remarkable total surface area, total pore volume and active cites generated from oxygen-containing functional groups on the surface of C-RFX/MWCNTs sample. The same observation was detected in the previous work [21] as result from a conventional carbonization of RFX/MWCNTs at 750ºC for 2h under N_2 gas flow. However, hydrothermal effect may contribute significantly to the enhancement in total surface area and generated oxygen functional groups as well as preserving a mesoporous structure with accessible adsorption sites for upgrading the adsorption efficiency towards CV dye from aqueous solutions.

3.3.5. Effect of initial dye concentration

The BTCs in Fig. 6 show the effect of initial influent CV concentrations of 50 and 25 mg/L at a bed height of 2cm and a solution flow rate of 5mL/min. As seen in Fig. 6, the breakthrough curve was flatter and actually occurred late for low influent concentrations of CV dye, and the surface of the three adsorbents was saturated after a long period of time, indicating a relatively film-controlled process. Whereas for higher influent concentration of CV dye, the breakthrough eventuated in a short period of time, signifying an intraparticle diffusion process [33]. These findings exhibit that the saturation rate and breakthrough time are affected by changes concentration gradient. This can be attributed to the fact that when the CV dye concentration increased, more adsorption sites were covered, allowing for quick breakthrough and exhaustion time. Table 2 displays that the inlet CV concentration increased, the percentage removal (%R) and t_b decreased.
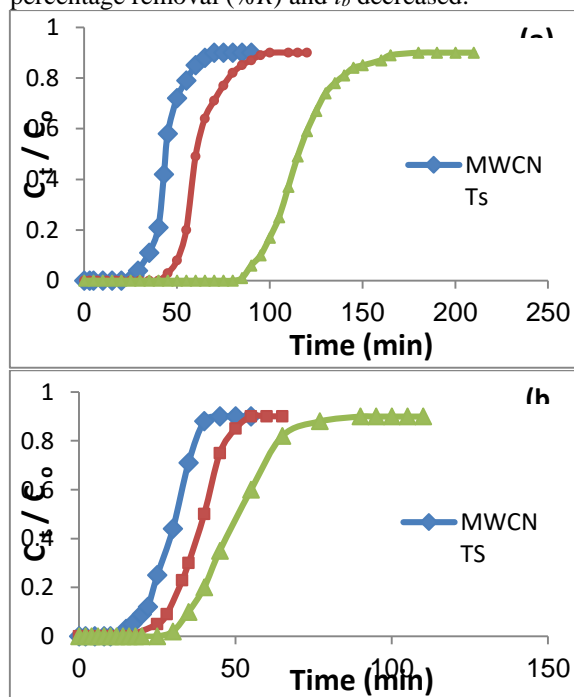

Figure 6: BTCs for the adsorption of CV by tested samples at different initial concentrations of (a) 25 and (b) 50 mg/L.

Table 2: Column data and parameters attained at various flow rate, bed height and inlet concentration.

	C_o (mg/L)	Z (cm)	Q (mL/min)	q_{total} (mg)	m_{total} (mg)	Total removal %	q_e (mg/g)	C_e (mg/L)	V_{eff}	t_{ex} (min)	T_b (min)
MWCNTs	25	2	5	2.6	8.1	32	13	1.5	325	65	25
	25	2	7	2.1	7.3	28	10	1.7	294	40	20
	25	1	5	1.5	6.3	24	10	2.3	200	40	5
	25	2	5	2.6	8.1	32	13	1.5	325	65	25
	25	2	5	2.6	8.1	32	19	2.1	200	65	25
	50	2	5	2.0	7.5	26	12.5	3.3	150	30	14
RFX/MWCNTs	25	2	5	3.0	13	25	16	1.9	500	100	40
	25	2	7	1.7	12	14	8.5	2.1	490	70	35
	25	1	5	1.2	6.2	19	6	2	250	50	20
	25	2	5	3	13	25	16	1.9	500	100	40
	25	2	5	3	13	25	16	1.9	500	100	40
	50	2	5	2	12	17	10	4.1	240	48	25
C-RFX/MWCNTs	25	2	5	10	23	43	50	2	900	180	85
	25	2	7	3.5	17	20	17.5	2	700	100	45
	25	1	5	2	8	28	20	1.8	325	65	35
	25	2	5	10	23	43	50	2	900	180	85
	25	2	5	10	23	43	50	2	900	180	85
	50	2	5	3	15	20	15	4	300	60	32

3.3.6. Application of column models

Wolborska and Adam-Bohart column sorption models were utilized to describe the initial part of BTCs applying experimental data. Table 3 shows the values of No, β and K_{AB} calculated from ln (C_t/C_o) against time (t, min) for all the investigated samples at various low rates, bed heights and influent concentrations of CV dye as well as the correlation coefficients (figures nit shown). The values of the kinetic constant (K_{AB}) at different flow rates decreased with the increase in flow rate while values of N_o and β increased with the increase in flow rate. For various CV dye concentrations in the inlet, the kinetic constant (K_{AB}), N_o and β reduced as the influent concentration of CV dye for MWCNTs sample increased. Whereas for RFX/MWCNTs and C-RFX/MWCNTs samples, with increase in the inlet CV dye concentration, the values of K_{AB} decreased while N_o and β values increased considerably. Additionally, at different bed heights, the values of K_{AB} decreased as the bed height increased from 1 to 2 cm. Meanwhile, the values of N_o and β decreased as the bed height increased for RFX/MWCNTs and C-RFX/MWCNTs samples; whilst increased for MWCNTs sample. This indicates that the overall system kinetic is controlled by external mass transfer in the initial part of adsorption in the column [34, 35]. The values of R^2 are lower according to Table 3, so the Wolborska and Adam-Bohart models were not advisable to be utilized in explaining the adsorption behavior of CV dye in a fixed bed column. Further, Clark model parameters and their correlation coefficient values are given in Table 4 and Fig. 7 a, b and c. It seems as influent CV dye concentration increased the value of r constant increased, while A value decreased with the increase of flow rate [35-37]. The correlation coefficient values (R^2) for the

obtained linear regression are adequate exhibiting good agreement of Clark model for describing the column adsorption performance of CV dye using the investigated adsorbents.
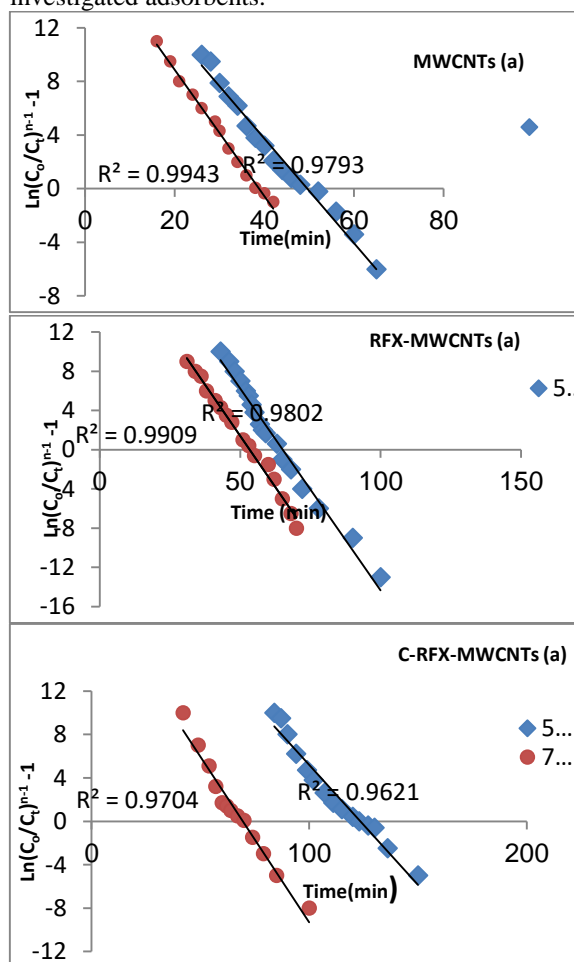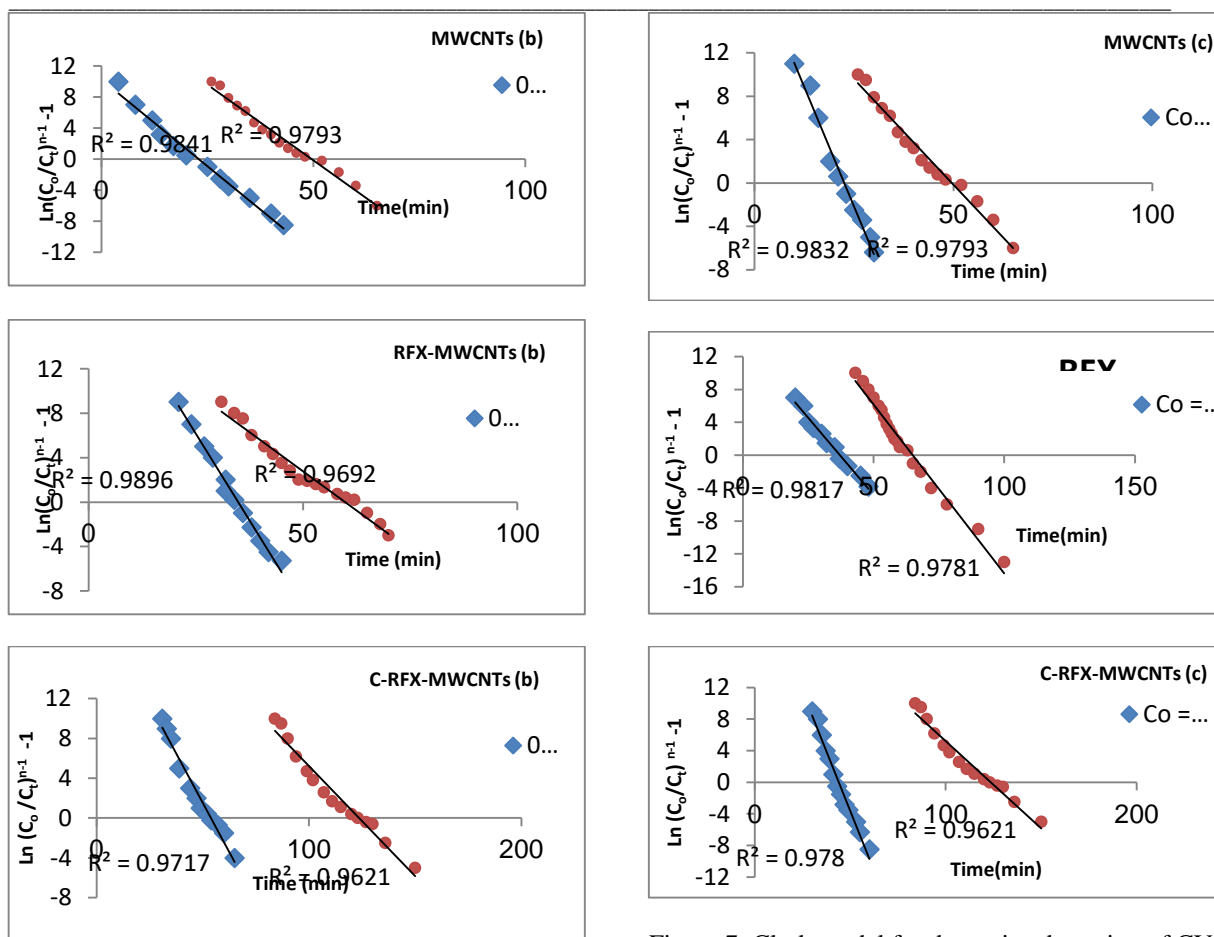
Figure 7: Clark modal for dynamic adsorption of CV at different (a) flow rate (b) bed height and (c) initial concentration.

Table 3 Adam-Bohart and Wolborska Parameters at various flow rate, bed height and inlet concentration

	MWCNTs				RFX/MWCNTs				C-RFX/ MWCNTs			
	Adam-Bohart		Wolborska		Adam-Bohart		Wolborska		Adam-Bohart		Wolborska	
C_o(mg/L)	K_{AB} (L/mg. min)	N_o (mg/L)	β (min^{-1})	R^2	K_{AB} (L/mg.min)	N_o (mg/L)	β (min^{-1})	R^2	K_{AB} (L/mg.min)	N_o (mg/L)	β (min^{-1})	R^2
25	0.34	3.9	0.03	0.83	0.35	4.2	0.03	0.86	0.32	2.0	0.05	0.85
50	0.3	0.05	4×10^{-3}	0.81	0.11	12.2	0.04	0.82	0.23	4.3	0.01	0.84
Z (cm)												
1	5.4	0.09	8×10^{-4}	0.80	0.28	19.4	0.24	0.84	0.34	8	0.05	0.82
2	0.34	3.9	0.03	0.83	0.35	4.2	0.03	0.81	0.32	2.0	0.05	0.85
Q(mL/min)												
5	0.34	3.9	0.03	0.83	0.35	4.2	0.03	0.86	0.32	2.0	0.05	0.85
7	0.32	14.6	0.75	0.82	0.25	6.0	0.2	0.81	0.3	4.4	0.02	0.82

Table 4 Clark parameters at various flow rate, bed height and inlet concentration

	MWCNTs			RFX/MWCNTs			C-RFX/ MWCNTs		
Q (mL/min)	**A**	**r**	**R^2**	**A**	**r**	**R^2**	**A**	**r**	**R^2**
5	3.0	0.14	0.97	3.2	0.26	0.98	3.5	0.14	0.96
7	2.3	0.13	0.99	2.5	0.21	0.99	2.5	0.17	0.97
C$_o$(mg/L)	**A**	**r**		**A**	**r**		**A**	**r**	
25	3.0	0.14	0.97	3.2	0.26	0.98	3.5	0.14	0.96
50	2.9	0.73	0.98	2.7	0.44	0.98	2.1	0.19	0.97
Z(cm)	**A**	**r**		**A**	**r**		**A**	**r**	
1	2.5	0.62	0.98	2.9	0.47	0.98	2.9	0.14	0.97
2	3.0	0.14	0.97	3.2	0.26	0.98	3.5	0.14	0.96

4. Conclusions

Three samples of multiwalled carbon nanotubes (MWCNTs), resorcinol-formaldehyde xerogel/CNTs (RFX/MWCNTs), and their carbonized sample via hydrothermal carbonization at 180oC for 3h (C-RFX/MWCNTs) were prepared and their adsorption performances in the removal of crystal violet dye using a fixed-bed mode were investigated in this research. When comparing C-RFX/MWCNTs to RFX/MWCNTs, the results showed that C-RFX/MWCNTs had more oxygenated functional groups and a significant increase in internal porosity. The adsorption bed capacity increased with increasing bed height, reducing flow rate, and decreasing initial dye concentration over the prepared samples, according to the outcomes of the column. However, the hydrothermally carbonized sample (C-RFX/MWCNTs) exhibited superior porous and column properties and thus this explained the significant impact of hydrothermal treatment on resorcinol- formaldehyde xerogel and carbon nanotubes nanohybrids.

Author's Declaration

Author's contributions

All the authors contributed equally in this work.

Conflict of interest

The authors declare that they have no known competing financial interests or personal relationships that could have appeared to influence the work reported in this paper.

References

[1] Pekala RW. Organic aerogels from the polycondensation of resorcinol with formaldehyde. J. Mater. Sci. 1989; 24: 3221–3227.

[2] Lin C, Ritter J A. Effect of synthesis pH on the structure of carbon xerogels. Carbon 1997; 35: 1271–1278.

[3] Wiener M, Reichenauer G, Braxmeier S, Ebert H P, Hemberger F. Carbon aerogel based high temperature thermal insulation. Int. J. Thermophys. 2009; 30: 1372–1385.

[4] Gao X, Omosebi A, Landon J, Liu K. Surface charge enhanced carbon electrodes for stable and efficient capacitive deionization using inverted adsorption – desorption behavior. Energy Environ. Sci. 2015; 8: 897–909.

[5] Girgis B S, Attia A A, Fathy N A. Potential of nano-carbon xerogels in the remediation of dye-contaminated water discharges. Desalination 2011; 265: 169–176.

[6] Pérez-Cadenas A F, Cornelia H R, Torres S M, Pérez-Cadenas M, Kooyman P J, Moreno-Castilla C, Kapteijn F. Metal-doped carbon xerogels for the electro-catalytic conversion of CO_2 to hydrocarbons. Carbon 2013; 56: 324–331.

[7] Fathy NA, El-Khouly SM, Aboelenin RMM. Carbon xerogel/Carbon Nanotubes Nanohybrid Doped with Ti for Removal of Methylene Blue Dye. Egypt. J. Chem. 2019; 62: 2277-2288.

[8] El-Khouly S, Fathy N. A review on nano-carbon materials for pollution remediation. Egypt. J. Chem. 2021; 64: 6929 - 6951.

[9] Attia AA, Shouman MA, Sayyah SM, Fathy NA, Khaliel AB, Abas KM. Sequestration of methylene blue and lead ions by MWCNT modified with polyconducting polymers. Egypt. J. Chem. 60 (2017) 221 –241.

[10] Fathy NA, El-Shafey S. Carbon-based nanohybrid fabricated in-situ and boosted the adsorption of anionic reactive yellow dye. Int. J. Environ. Sci. Technol. 2022. https://doi.org/10.1007/s13762-022-04061-7.

[11] Tabrizi NS, Yavari M. Methylene blue removal by carbon nanotube-based aerogels. Chem. Eng. Res. Design 2015; 94: 516–523.

[12] Worsley MA, Satcher JH, Baumann TF. Synthesis and characterization of monolithic carbon aerogel nanocomposites containing double-walled carbon nanotubes. Langmuir 2008; 24: 9763–9766.

[13] Worsley MA, Pauzauskie PJ, Kucheyev SO, Zaug JM, Hamza AV, Satcher JH, Baumann TF. Properties of single-walled carbon nanotube-based aerogels as a function of nanotube loading. Acta Mater. 2009; 57: 5131–5136.

[14] Haghgoo M, Yousefi AA, Mehr MJZ, Celzard A, Fierro V, Léonard A, Job N. Characterization of multi-walled carbon nanotube dispersion in resorcinol–formaldehyde aerogels. Micropor. Mesopor. Mater. 2014; 184: 97–104.

[15] Haghgoo M, Yousefi AA, Mehr MJZ, Léonard AF, Philippe MP, Compére P, Léonard A, Job N. Correlation between morphology and electrical conductivity of dried and carbonized multi-walled carbon nanotube/resorcinol – formaldehyde xerogel composites. J. Mater. Sci. 2015; 50: 6007–6020.

[16] Fathy NA, Annamalai KP, Tao Y. Effects of phosphoric acid activation on the nanopore structures of carbon xerogel/carbon nanotubes hybrids and their capacitance storage. Adsorption 2017; 23: 355–360.

[17] Fernández PS, Castro EB, Real SG, Visintin A, Arenillas A, Calvo EG, Juárez-Pérez EJ, A.J. Menéndez, Martins ME, Electrochemical behavior and capacitance properties of carbon

xerogel/multiwalled carbon nanotubes composites. J. Solid State Electrochem. 2012; 16: 1067–1076.

[18] Ordeñana-Martínez AS, Rincón ME, Vargas M, Estrada-Vargas A, Casillas N, Bárcena-Soto M, Ramos E. Carbon nanotubes/carbon xerogel-nafion electrodes: a comparative study of preparation methods. J. Solid State Electrochem. 16 (2012) 3777–3782.

[19] Shouman MA, Fathy NA. Microporous nanohybrids of carbon xerogels and multi-walled carbon nanotubes for removal of rhodamine B dye. J. Water Proc. Eng. 2018; 23:165–173.

[20] Fathy NA. Carbon nanotubes synthesis using carbonization of pretreated rice straw through chemical vapor deposition of camphor. RSC Adv. 2017; 7: 28535–28541.

[21] Fathy N, Lotfy V, Basta A. Comparative study on the performance of carbon nanotubes prepared from agro- and xerogels as carbon supports. J. Anal. Appl. Pyrol. 2017; 128: 114–120.

[22] Rabjeshkannan R, Rajasimman M, Rajamohan N. Packed bed column studies for the removal of dyes using novel adsorbent. Chem Ind. Chem. Eng. Quart 2013; 19: 467-470.

[23] Zeng P, Bai B, Guan W, Wang H, Suo Y. Fixed bed column studies for the removal of anionic dye from aqueous solution using TiO_2@glucose carbon composites and bed regenration study. J. Mater. Electron 2016; 27: 867-877.

[24] Yu J-X, Zhu J, Feng L, Cai X, Zhang Y, Chi R. Removal of cationic dyes by modified waste biosorbent under continuous model: Competitive adsorption and kinetics. Arab. J. Chem. 2019; 12: 2044-2051.

[25] Wolborska A. Adsorption on activated carbon of p-nitrophenol from aqueous solution. Water Res. 1989; 23: 85-91.

[26] Shanmugam D, Alagappan M, Rajan R K. Bench-scale packed bed sorption of Cibarcron blue F3GA using lucrative algal biomass. Alex Eng. J. 2016; 55: 2995-3003.

[27] Clark RM. Evaluating the cost and performance of field-scale granular carbon systems. Environ. Sci. Technol. 1987; 21: 573-580.

[28] Chowdhury ZZ, AbdHamid SB, MohZain S. Evaluating design parameters for breakthrough curves analysis and kinetics of fixed bed columns for Cu(II) cations using lignocellulosic wastes. Bioresources 2015; 10: 732-749.

[29] Attia A, Shouman M, Khedr SA, Fagel GA. Removal of chromium (VI) from wastewater via polyvinyl alcohol and polyvinyl alcohol/chitosan encapsulated onto Jojoba leaves:Fixed-bed column studies. Desalin. Water Treat. 2020; 190: 203-214.

[30] Zhang J, Zou H, Qing Q, et al. Effect of chemical oxidation on the structure of single-walled carbon nanotubes. J Phys Chem B. 2003; 107: 3712–3718.

[31] Bharathi KS, Ramesh ST. Fixed bed column studies on biosorption of crystal vioelt from aqueous solution by Citrullus lanatus rind and Cyperus rotundus. Appl. Water Sci. 2013; 3: 673-687.

[32] Attia A, Shouman M, Khedr S, Hassan N. Fixed-bed column studies for the removal of congo red using Simmonlosia Chinesis (Jojoba) and coated with chitosan. Indones. J. Chem. 2018; 18: 294-305.

[33] Aktar M, Khan SU, Mozhar N, Naveed M, Yasir QM, Ahmed W. Optimization of crystal violet dye removal in fixed bed column using Eucalyptus camaldulensis as a low-cost adsorbent. Letters Appl. NanoSci. 2022; 11: 4114-4130.

[34] Lopez-Cervantes J, Sanchez-Machado DI, Sanchez-Duarte RG, Correa-Murrieta M.A. Study of a fixed-bed column in the adsorption of an azo dye from an aqueous medium using a chitosan–glutaraldehyde biosorbents. Adsorp. Sci Technol. 2018; 36: 215-232.

[35] Lin X, Li R, Wen Q, Wu J, Fan J, Jin X, Qian W, Liu D, Chen X, Chen Y, Xie J, Bai J, Ying H. Experimental and modeling studies on the sorption breakthrough behaviors of butanol from aqueous solution in a fixed-bed of KA-I resin. Biotechnol. Bioproc. Eng. 2013; 18: 223–233.

[36] Negrea A, Mihailescu M, Mosoarca G, Ciopec M, Duteanu N, Negrea P, Minzatu V. Estimation on fixed-bed column parameters of breakthrough behaviors for gold recovery by adsorption onto modified/functionalized Amberlite XAD7. Int. J. Environ. Res. Public Health 2020; 17: 6868.

[37] Afroze S, Kanti ST, Ang HM. Adsorption performance of continuous fixed bed column for the removal of methylene blue (MB) dye using Eucalyptus sheathiana bark biomass. Res. Chem. Intermediates 2016; 42: 2343–2364